Macrocyclic Hosts for Fullerenes: Extreme Changes in Binding Abilities with Small Structural Variations.

David Canevet,[†] María Gallego,[‡] Helena Isla,[‡] Alberto de Juan,[‡] Emilio M. Pérez,[*,†,‡] and Nazario Martín[*,†,‡]

[†]IMDEA-Nanociencia, Facultad de Ciencias, Ciudad Universitaria de Cantoblanco, E-28049 Madrid, Spain
[‡]Departamento de Química Orgánica, Facultad de Química, Universidad Complutense de Madrid, E-28040 Madrid

S *Supporting Information*

ABSTRACT: Exploiting the shape and electronic complementarity of C_{60} and C_{70} with π-extended derivatives of tetrathiafulvalene (exTTF), we have very recently reported a macrocyclic receptor featuring two exTTF recognizing units which forms 1:1 complexes with C_{60} with log K_a = 6.5 ± 0.5 in chlorobenzene at 298 K. This represents one of the highest binding constants toward C_{60} reported to date and a world-record for all-organic receptors. Here, we describe our efforts to fine-tune our macrocyclic bis-exTTF hosts to bind C_{60} and/or C_{70}, through structural variations. On the basis of preliminary molecular modeling, we have explored p-xylene, m-xylene, and 2,6-dimethylnaphthalene as aromatic spacers between the two exTTF fragments and three alkene-terminated chains of different length to achieve macrocycles of different size through ring closing metathesis. Owing to the structural simplicity of our design, all nine receptors could be accessed in a synthetically straightforward manner. A thorough investigation of the binding abilities of these nine receptors toward C_{60} and C_{70} has been carried out by means of UV−vis titrations. We have found that relatively small variations in the structure of the host lead to very significant changes in affinity toward the fullerene, and in some cases even in the stoichiometry of the associates. Our results highlight the peculiarities of fullerenes as guests in molecular recognition. The extreme stability of these associates in solution and the unique combination of electronic and geometrical reciprocity of exTTF and fullerenes are the main features of this new family of macrocyclic hosts for fullerenes.
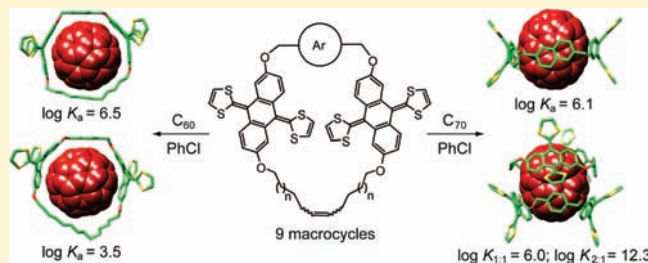
1. INTRODUCTION

The search for molecular receptors for fullerenes was initiated soon after their discovery[1] with the pioneering work of the groups of Diederich, Ringsdorf, and Wennerström.[2] The main motivations that have kept it as a very active area of research[3,4] are the selective association of specific fullerenes to achieve their purification from complex mixtures[3g,3q,3r] and the construction of organized electroactive nanostructures by self-assembly.[4] In both cases the formation of associates with fullerenes of high stability in solution—that is, the construction of hosts that show large binding constants toward the fullerenes—is one of the main goals. To achieve this objective, a broad variety of molecular fragments capable of establishing positive noncovalent interactions with the outer surface of fullerenes have been explored. These include derivatives of calix[n]arenes,[3b,3j,3n,5] cyclotriveratrylenes,[3q,3r,6] corannulenes,[3p,7] cyclic paraphenyleneacetylenes,[8] π-extended tetrathiafulvalenes,[3h,3l,3o,3t] and, most frequently, porphyrins.[3c,3s,3v,9]

Although the experimental results from different groups are sometimes difficult to compare due to the use of different methods to assess the binding constants and to the different solvents utilized, taking C_{60} as a reference fullerene guest, it is fair to say that obtaining hosts that show binding constants of log K_a = 5 or larger remains a major challenge. Aida's bisporphyrin macrocycles—in which porphyrin units are connected via flexible alkyl spacers—constitute perhaps the most successful family of hosts for fullerenes

to date.[3c,3s,3v,9a,9b,9f] For example, the Zn(II) metalloporphyrin congener shows a log K_a = 5.8 toward C_{60}, while the free base shows log K_a = 5.9, both in benzene at room temperature.[9f] The world-record in complex stability is the Ir(III) metalloporphyrin derivative which shows a log K_a = 8.1 for C_{60} in 1,2-dichlorobenzene (o-DCB) at room temperature.[3s] It is noteworthy that in the latter case, the authors indicate that the supramolecular nature of the host−guest system is arguable, since iridium was found to bind a 6,6 junction of the fullerene in a η^2 fashion. Recently, a macrocycle featuring three porphyrins[10] and a "nanobarrel" formed by four porphyrin units[11] have been shown to bind C_{60} with log K_a = 6.2 and 5.7, respectively, both in toluene at room temperature.
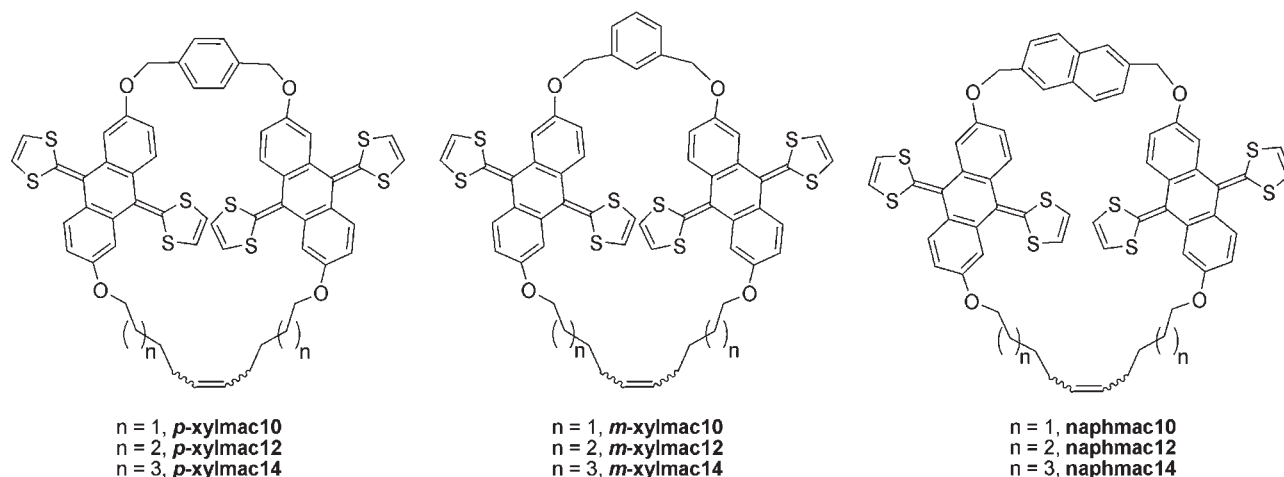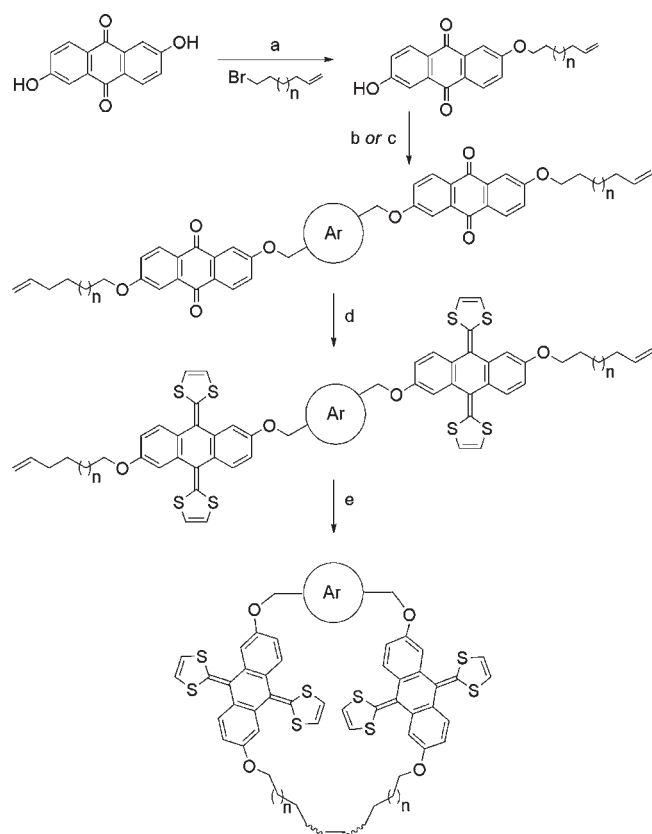
2. DESIGN AND SYNTHESIS

We have very recently reported a macrocyclic receptor that associates C_{60} with log K_a = 6.5 ± 0.5 in PhCl at room temperature (p-xylmac12 in Chart 1).[12] The design of the macrocyclic host was based on our initial tweezers-like receptors, in which two exTTF units were connected through an isophthalic diester spacer. This simple receptor served as proof-of-principle for the utilization of exTTF as recognizing motif in the construction of hosts for fullerenes, and showed respectable affinities toward C_{60}

Chart 1. Chemical structures of the nine receptors

n = 1, **p-xylmac10**
n = 2, **p-xylmac12**
n = 3, **p-xylmac14**

n = 1, **m-xylmac10**
n = 2, **m-xylmac12**
n = 3, **m-xylmac14**

n = 1, **naphmac10**
n = 2, **naphmac12**
n = 3, **naphmac14**

Scheme 1. General Scheme for the Synthesis of the Macro-cyclic Hosts[a]

[a] Conditions: (a) K_2CO_3, NaI (cat.), DMF, reflux; (b) for **p-xylmac** and **m-xylmac** families, α,α'-p-dibromoxylene, or α,α'-m-dibromoxylene, K_2CO_3, NaI (cat.), DMF, 60 °C; (c) for **naphmac** family, 2,6-bis(hydroxymethyl)naphthalene, Ph_3P, diethyl azodicarboxylate, THF, reflux; (d) dimethyl 1,3-dithiol-2-ylphosphonate, BuLi, THF, −78 °C to room temp; (e) Grubb's first generation catalyst, CH_2Cl_2, room temp.

considering its lack of preorganization (log K_a = 3.5 in PhCl at room temperature).[3t] To increase the degree of preorganization,

we conserved all the basic traits of the exTTF tweezers, but included an alkyl linker with terminal alkenes to achieve macrocyclization through RCM. In the present study, we describe a collection of macrocyclic hosts with systematic structural modification of both the alkyl and aromatic spacers. Considering the precedents and preliminary molecular modeling, we decided to investigate p-xylene, m-xylene and 2,6-dimethylnaphthalene as aromatic spacers, and hexene, heptene and octene as alkyl spacers and precursors for RCM. The structures of the receptors synthesized are shown in Chart 1. The nomenclature utilized identifies the aromatic spacer and the length of the alkenyl spacers.

The **p-xylmac** and **m-xylmac** families (n = 1−3) were synthesized following a procedure analogous to that reported for **p-xylmac12** (Scheme 1).[12] The synthesis starts with the Williamson etherification of anthraflavic acid with the corresponding bromoalkene under standard conditions, followed by dialkylation of either para or meta-α,α'-dibromoxylene with the remaining phenolic OH, which yielded linear tetraketone precursors. These were subjected to Horner−Wadsworth−Emmons olefination with dimethyl 1,3-dithiol-2-ylphosphonate, to afford the bis-exTTF linear precursors, which were finally treated with Grubb's first generation catalyst to obtain the desired macrocycles. The synthesis of the **naphmac** family follows the same procedure, but utilizing 2,6-bis(hydroxymethyl)naphthalene and a Mitsunobu protocol to obtain linear bis-anthraquinone precursors (Scheme 1). This was followed by olefination to form the exTTF derivatives and RCM to yield the macrocycles as a chromatographically inseparable mixture of E/Z isomers, which was used as such. The identity and purity of the nine macrocyclic hosts and all synthetic intermediates were unambiguously established by standard spectroscopic and analytical techniques (see the Supporting Information for full experimental details and characterization).

3. ASSOCIATION OF C_{60} AND C_{70}

Binding constants were estimated through UV−vis titrations. In a typical experiment, we prepared stock solutions of the macrocyclic receptor in PhCl at a concentration approximately equal to the reciprocal of the binding constant. Those solutions were utilized as solvents in the solution of fullerene, to ensure working at constant concentration of host. Aliquots of the fullerene solution were
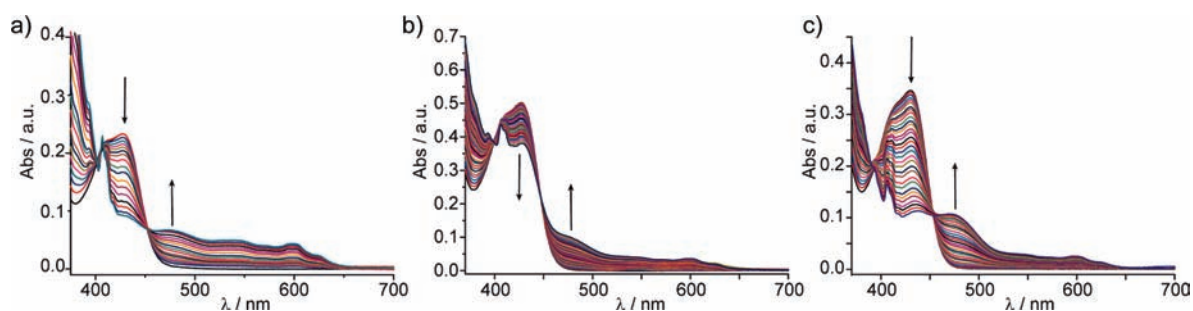
Figure 1. Spectral changes in UV−vis titration experiments of (a) *p*-xylmac12, (b) *m*-xylmac12, and (c) **naphmac12** against C_{60} in PhCl at 298 K.

Table 1. Logarithm of the Calculated Binding Constants for the Macrocyclic Hosts towards C_{60} and C_{70}, as Estimated from Three Separate UV−vis Titration Experiments in PhCl at 298 K

	C_{60}	C_{70}
p-xylmac10	4.3 ± 0.5	6.0 ± 0.4; 12.3 ± 0.6[a]
p-xylmac12	6.5 ± 0.5	b
p-xylmac14	3.5 ± 0.6	5.9 ± 0.3
m-xylmac10	4.0 ± 0.5	4.4 ± 0.4; 8.3 ± 0.5[a]
m-xylmac12	4.8 ± 0.4	b
m-xylmac14	4.1 ± 0.4	5.4 ± 0.3
naphmac10	4.0 ± 0.2	4.7 ± 0.3
naphmac12	5.6 ± 0.6	5.6 ± 0.4
naphmac14	3.4 ± 0.1	6.1 ± 0.2

[a] First binding constant corresponds to $\log K_{1:1}$ and second to $\log K_{2:1}$.
[b] Titration data did not provide satisfactory fits (see main text).

added to the host solution until reaching 3−4 mol equiv, and UV−vis spectra recorded at room temperature on a Cary UV-50 or on a Shimadzu UV-3600 spectrophotometer equipped with a temperature control unit. Analysis of the UV−vis data to determine binding constants was carried out utilizing Specfit multivariable analysis software. Experiments were repeated three times. The values of the binding constants are reported in Table 1 and were calculated as the mean value of the three experiments, with the error estimated as the standard deviation.

The changes in the absorption spectra during the titrations against C_{60} are very similar for all nine receptors. As representative examples, Figure 1 shows the evolution of the spectra of the best host of each series, *p*-xylmac12, *m*-xylmac12, and **naphmac12** upon increasing C_{60} concentration. In all cases, we observe the decrease in absorption of the band at $\lambda_{max} \approx 425-430$ nm, and the appearance of a charge-transfer band at $\lambda_{max} \approx 470-475$ nm. An isosbestic point at around 450 nm is also clearly observable. These spectral changes distinctively indicate association of C_{60} inside the cavity of the macrocycle.[12] The relative intensity of the changes correlates very well with the calculated binding constants (see Figure 1). For *p*-xylmac12 ($\log K_a = 6.5 \pm 0.5$) and **naphmac12** ($\log K_a = 5.6 \pm 0.6$) both the decrease in the absorption of the exTTF and the increase in absorption of the charge-transfer band are significantly more marked than for *m*-xylmac12 ($\log K_a = 4.8 \pm 0.4$).

The titration data versus C_{60} for all nine macrocycles were fitted successfully to a 1:1 binding mode,[13] yielding the binding constants summarized in Table 1. From the values of the binding constants, it is clearly apparent that the *m*-xylylene spacer is the least adequate of the aromatics, with *p*-xylylene producing the
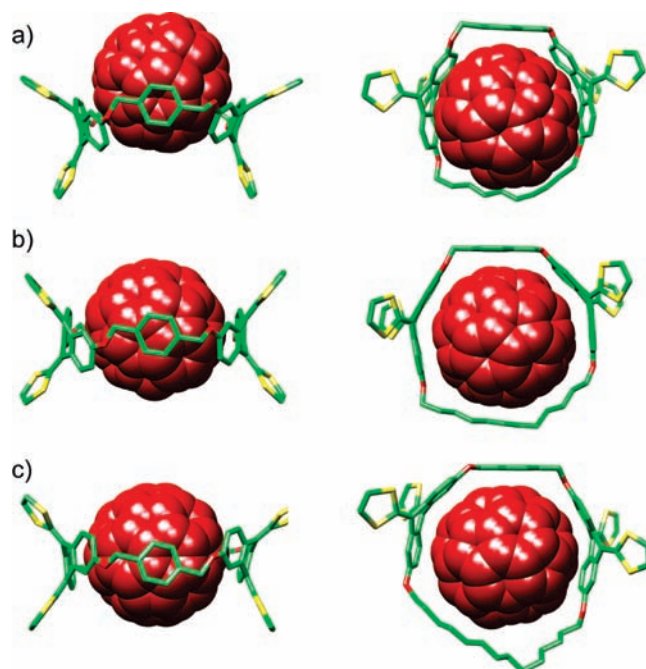

Figure 2. Side and top views of the energy-minimized (AMBER) models of the associates: (a) *p*-xylmac10·C_{60}; (b) *p*-xylmac12·C_{60}; (c) *p*-xylmac14·C_{60}. The macrocycles are depicted in stick representation with carbon atoms in green, sulfurs in yellow, and oxygens in red. Hydrogen atoms are not shown for clarity. [60]Fullerenes are depicted as space-filling models and colored in dark red.

best host for C_{60}, and naphthalene in an intermediate position. With regards to the alkyl spacer, the C_{12} derivative consistently shows the highest binding constant, with a very significant increase compared to C_{10} (too small) and C_{14} (too large). These results are qualitatively well reproduced by molecular mechanics calculations in the gas phase.[14] Figure 2 shows the geometry optimized models for the *p*-xylmac series to illustrate this point.

In *p*-xylmac10·C_{60} (Figure 2a) the macrocyclic cavity is too small to associate C_{60}, and the host adopts a bowl-type conformation, accommodating the fullerene above the plane of the macrocycle. In contrast, in *p*-xylmac12·C_{60} (Figure 2b) C_{60} fits perfectly inside the cavity of the macrocycle, with both exTTF units, the aromatic linker, and the alkyl spacer closely wrapping the fullerene unit. Finally, C_{60} fits loosely in *p*-xylmac14, so only part of the alkyl chain can approach the [60]fullerene and provide stabilizing van der Waals interactions.

The evolution of the spectra during the titrations against C_{70} is much less uniform across the different families of macrocycles

attending to the aromatic spacer. The spectral changes in the **naphmac** series mirror what we have previously observed for exTTF-cyclotriveratrylene hosts,[3h] namely, during the first additions the absorbance at $\lambda_{max} = 430$ nm decreases, with the concomitant increase of a charge-transfer band centered at $\lambda = 471$ nm. As the concentration of C_{70} increases the spectral changes become difficult to trace due to spectral overlap. Figure 3 depicts the experimental results obtained in the titration of **naphmac14** vs C_{70} (PhCl, 298 K). All three titrations for **naphmac10**, **naphmac12**, and **naphmac14** fitted successfully to a 1:1 binding model (see Figure 3 inset), yielding larger binding constants as the size of the macrocyclic cavity increases (see Table 1), as could be expected. Thus, the most efficient binder for C_{70} was found to be **naphmac14**, with a remarkable binding constant of log $K_a = 6.1 \pm 0.2$.

On the other hand, the **p-xylmac** and **m-xylmac** families showed parallel trends, depending on the length of the alkyl spacer. The larger members of each series, **p-xylmac14** and **m-xylmac14** behaved similarly to the **naphmac** hosts, and analysis of their titration data was performed satisfactorily utilizing a 1:1 binding model, yielding binding constants of log $K_a = 5.9 \pm 0.3$ and 5.4 ± 0.3, for **p-xylmac14** and **m-xylmac14**, respectively.

Unexpectedly, the smaller macrocycles **p-xylmac10** and **m-xylmac10** showed singular spectroscopic changes during the titration experiments. Figure 4a shows the variations in the electronic absorption spectrum of **p-xylmac10** upon additions of 0.1 equiv aliquots of C_{70} in PhCl at 298 K. Although at first sight the general trends are similar to those we observed for **naphmac** hosts (see Figure 3), a closer look at the titration data
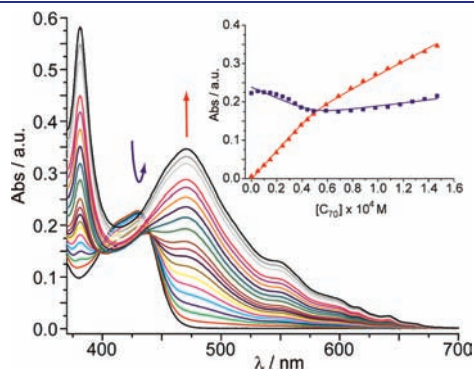
offers major and informative differences. During the first three additions of the titration, where the concentration of the macrocycle is significantly larger than that of the [70]fullerene, two very well-defined isosbestic points at $\lambda = 402$ and 432 nm can be noted (Figure 4b, inset). As the concentration of C_{70} increases these isosbestic points are lost, indicating the coexistence of more than one type of associates in solution. All these features point to the formation of complexes of both 2:1 and 1:1 host/guest stoichiometry, with the former prevailing in the early stages of the titration, and complexes of both stoichiometries being present in solution when the concentration of C_{70} increases sufficiently. Indeed, the titration data did not provide satisfactory fits when assuming either a 1:1 or a 2:1 stoichiometry exclusively. On the contrary, the multivariable analysis software converged nicely when we utilized a model where both types of associates are presumed to exist in solution (Figure 4a, inset). The calculated binding constants for **p-xylmac10** were log $K_{1:1} = 6.0 \pm 0.4$ and log $K_{2:1} = 12.3 \pm 0.6$, in agreement with both types of associates showing similar stability. Analogously, we estimated log $K_{1:1} = 4.4 \pm 0.4$ and log $K_{2:1} = 8.3 \pm 0.5$ for **m-xylmac10**, which also shows smaller binding constants toward C_{70}, as was the case with C_{60}. Conclusive evidence for this model was provided by Job's plot analysis, which showed a broad maximum centered at a molar fraction of 0.3−0.45 (Figure 4c), in an intermediate situation between 2:1 and 1:1, where the maxima would be located at 0.33 and 0.5, respectively.

Finally, **p-xylmac12** and **m-xylmac12** are apparently left in an intermediate situation between the C_{10} and C_{14} members, and, although association of C_{70} seems to take place considering the spectral changes, we could not achieve correct fitting of their titration data with any binding model. For instance, for **m-xylmac12** the best fit was obtained with a 1:1 model, and yielded a clearly overestimated binding constant of log $K_a = 9.9 \pm 2.6$, with excessive error and less than modest fitting for the binding isotherms (Figure 5). Similarly, the best fit for the data corresponding to **p-xylmac12** vs C_{70} affords log $K_a = 8.4 \pm 2.5$.[12]

As with C_{60}, the experimental results can be rationalized in terms of a simple lock and key model through molecular mechanics calculations. The energy-minimized models of **p-xylmac10**·C_{70} and **naphmac10**·C_{70} are shown in Figure 6 structures a and c. The cavity of **p-xylmac10** is too small to accommodate C_{70}, and leaves a significant part of its ellipsoidal surface exposed, so that it can be bound by another molecule of the host (Figure 6b) without steric congestion. On the other hand, the slight increase in size provided by the naphthalene spacer in **naphmac10** is sufficient to allow C_{70} to penetrate deeper into its cavity, stabilizing the 1:1 associate
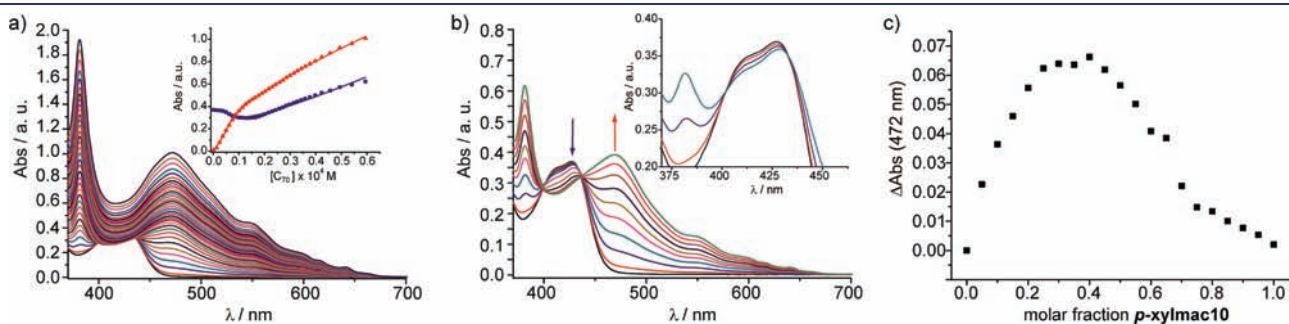

Figure 3. UV−vis spectra as recorded during the titration of **naphmac14** vs C_{70} (PhCl, 298 K). Inset shows the binding isotherms at 430 nm (blue squares) and 471 nm (red triangles); solid lines represent the fits. For this particular experiment a log $K_a = 6.0$ was calculated.

Figure 4. (a) UV−vis spectra as recorded during the titration of **p-xylmac10** vs C_{70} (PhCl, 298 K). Inset shows the binding isotherms at 430 nm (blue squares) and 472 nm (red triangles), solid lines represent the fits. (b) First 10 additions, up to 1 equiv of C_{70}. Inset shows the first three additions. (c) Job's plot ([**p-xylmac10**] + [C_{70}] = 1.0×10^{-4} M).

3187

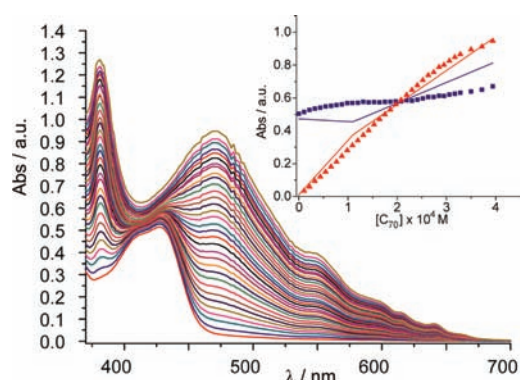dx.doi.org/10.1021/ja111072j |J. Am. Chem. Soc. 2011, 133, 3184–3190

Figure 5. UV–vis spectra as recorded during the titration of *p*-**xylmac12** vs C_{70} (PhCl, 298 K). Inset shows the binding isotherms at 430 nm (blue squares) and 471 nm (red triangles); solid lines represent the fits.
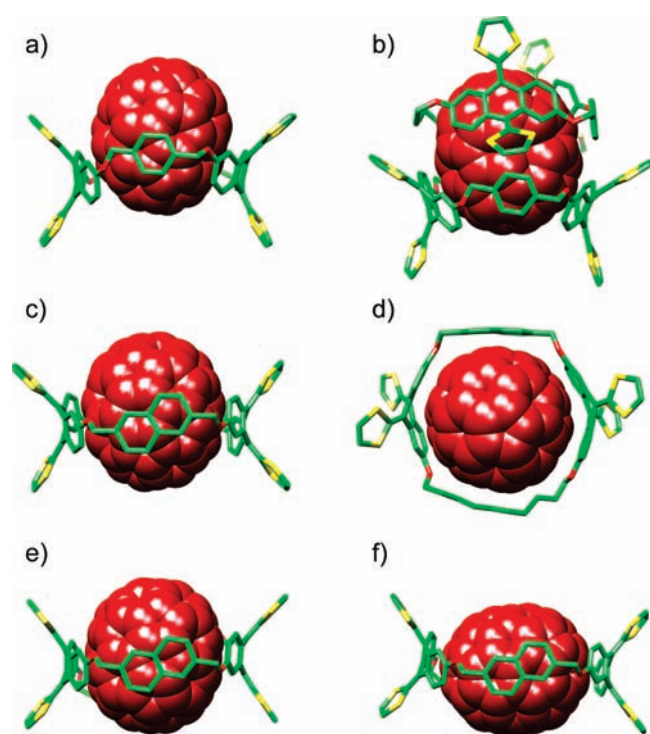

Figure 6. Energy-minimized (AMBER) models of the associates: (a) *p*-**xylmac10**·C_{70}; (b) *p*-**xylmac10**·C_{70}·*p*-**xylmac12**; (c) **naphmac10**·C_{70}, side view and (d) top view; (e) **naphmac14**·C_{70} with the guest perpendicular to the plane of the macrocycle; (f) **naphmac14**·C_{70} with the guest parallel to the plane of the macrocycle. The macrocycles are depicted in stick representation with carbon atoms in green, sulfurs in yellow, and oxygens in red. Hydrogen atoms are not shown for clarity. [70]Fullerenes are depicted as space-filling models and colored in dark red.

(Figure 6c,d). Meanwhile, **naphmac14** is the only macrocycle which is large enough to be capable of hosting C_{70} with its longer axis parallel to the plane of the macrocycle (Figure 6f). This provides an alternative to the perpendicular binding we observe for all other macrocycles, and can be responsible for the increase in stability.

To complete our understanding of the recognition process of these macrocyclic systems and gain an insight into its thermodynamic nature, we carried out titrations at different temperatures (288, 298, 308, and 318 K) in PhCl. As model system, we
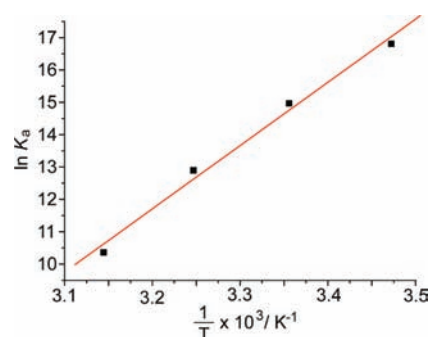

Figure 7. Plot of the natural logarithm of K_a vs $1/T$ for the association of C_{60} with *p*-**xylmac12** in PhCl.

chose the best binder of the family: *p*-**xylmac12** and C_{60} as a host. A plot of the natural logarithm of K_a vs $1/T$ is shown in Figure 7. The data show a clear linear tendency and was fitted to a straight line ($r^2 = 0.995$) with a slope of 19557 ± 1416 and an intercept of -51 ± 5. From these data, the standard enthalpy of association was calculated to be $\Delta H° = -163 \pm 12$ kJ mol^{-1} (-38 ± 3 kcal mol^{-1}) and $\Delta S° = -424 \pm 42$ J mol^{-1} (-101 ± 10 cal mol^{-1}). Thus, the association of fullerenes by our exTTF-based macrocyclic hosts is driven by strong enthalpic interactions. For comparison, the enthalpy value is approximately two to three times higher than that calculated for the association of C_{60} by calix[4]naphthalenes in toluene, which show a log $K_a = 2.8$.[15]

The appearance of a charge-transfer band during the titration suggests that electronic interactions between the fullerenes and our bis-exTTF macrocycles take place. These interactions in the ground state are also noticeable in cyclic voltammetry (CV) experiments. Though adsorption phenomena prevent a reliable measure of the oxidation potential of exTTF units, the cathodic part of the CV allowed us to draw interesting conclusions. Figure 8a shows the CVs of *p*-**xylmac12** (black), C_{60} (blue), and a mixture of both compounds (red). In the presence of a macrocycle, the half-wave potentials associated with the reduction signals of [60]fullerene are clearly shifted, which definitely confirms an interaction in the ground state between the host and the guest, even though both positive and negative shifts were detected. Similar measurements (Figure 8b), performed with **naphmac14** and C_{70}, indicate a strong electronic communication in the complex with a half-wave potential shift as high as -150 mV for the fourth reduction of C_{70}.

To further investigate the influence of the electronic communication on the stability of the complexes, we carried out titrations in solvents of different polarities. In the more polar benzonitrile ($\varepsilon_r = 25.2$), where charge-transfer interactions should be favored, we calculated a binding constant of log $K_a = 7.5 \pm 0.9$. The increase in binding constant cannot be ascribed solely to stabilization of the complex through enhanced charge-transfer interactions, since the solubility of C_{60} in benzonitrile is 0.4 mg/mL. This is conclusively confirmed in the nonpolar toluene ($\varepsilon_r = 2.4$), in which a decrease in binding constant to log $K_a = 5.4 \pm 0.9$ was found. Considering the decrease in solubility of C_{60} when moving from chlorobenzene (6.4 mg/mL) to toluene (2.4 mg/mL)[16] this is evidence of the contribution of the electronic interactions to the stabilization of the *p*-**xylmac12**·C_{60} associate, since a decrease in binding constant with increasing solubility is typically found.[3u] Such effect can be attributed to the solvation penalty associated with the formation of the
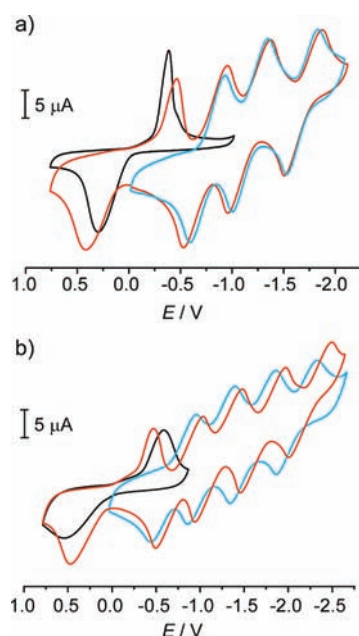
Figure 8. Cyclovoltammograms of (a) *p*-**xylmac12** (black), C$_{60}$ (blue), and *p*-**xylmac12**·C$_{60}$ (red); (b) **naphmac14** (black), C$_{70}$ (blue), and **naphmac14**·C$_{70}$ (red), in PhCl, Bu$_4$NClO$_4$ (0.1 M), ν = 0.1 V s^{-1}, [fullerene] = [macrocycle] = 5 × 10^{-4} M. Potentials are indicated vs the Ag/AgNO$_3$ redox couple.

supramolecular assembly. Since a significant portion of the molecular surfaces of both the receptor and the guest becomes unavailable for solvation upon complexation, the solvation penalty is more severe in solvents which solvate the separated entities more efficiently.

4. CONCLUSIONS

We have synthesized a collection of nine macrocycles bearing two units of exTTF as recognition elements for the fullerenes, connected through three different aromatic and alkyl spacers, and investigated their binding abilities toward C$_{60}$ and C$_{70}$. It was found that *p*-**xylmac12** is the best binder for C$_{60}$ with log K_a = 6.5 ± 0.5 for C$_{60}$ in PhCl and log K_a = 7.5 ± 0.9 in benzonitrile. These values make *p*-**xylmac12** one of the most efficient receptors for C$_{60}$ reported to date. With regards to C$_{70}$, **naphmac14** and *p*-**xylmac14** show log K_a = 6.1 ± 0.2 and 5.9 ± 0.3, respectively, in PhCl at 298 K. These are two of the very few examples of hosts capable of associating C$_{70}$ with micromolar affinity.[3h,17] From the general point of view of the design of hosts for fullerenes, our results show that relatively small structural variations in the receptor lead to large changes in binding affinities, and in, some cases, even stoichiometry. For example, while *m*-**xylmac14** forms 1:1 complexes with C$_{70}$ with a respectable binding constant of log K_a = 5.4 ± 0.3, the smaller member *m*-**xylmac10** forms associates of both 1:1 and 2:1 stoichiometries, with log $K_{1:1}$ = 4.4 ± 0.4 and log $K_{2:1}$ 8.3 ± 0.5. With regards to C$_{60}$, an impressive change in binding constant of nearly 3 orders of magnitude is found when moving from *p*-**xylmac12** (log K_a = 6.5 ± 0.5) to *p*-**xylmac14** (log K_a = 3.5 ± 0.6). These differences underline the singularities of fullerenes as hosts in molecular recognition and highlight the importance of fine-tuning the structure of the receptors. Remarkably, all our experimental results can be qualitatively explained with

a simple lock and key model through undemanding molecular mechanics calculations.

To shed light on the driving force for binding, we have determined the thermodynamic parameters for the formation of *p*-**xylmac12**·C$_{60}$. To that end, we have carried out titrations at different temperatures (318, 308, 298, and 288 K). The positive slope of the ln K_a vs $1/T$ indicates that association is driven by enthalpy. Indeed, we calculated a remarkably high $\Delta H°$ = −163 ± 12 kJ mol^{-1} (−38 ± 3 kcal mol^{-1}). The spectral features observed during the UV−vis titrations, cyclic voltammetry data, and titrations carried out in solvents of different polarity suggest that electronic interactions between the exTTF and C$_{60}$ contribute significantly to the stabilization of the complex.

In the near future, we plan to exploit the extreme stability of the bis-exTTF macrocycle−fullerene complexes, the lessons extracted from the structure−affinity relationships, and the relatively simple synthetic access to the macrocycles to construct chiral hosts for the enantioselective molecular recognition of the inherently chiral higher fullerenes.[3g,3v]

■ ASSOCIATED CONTENT

ⓢ Supporting Information. Supplementary figures, characterization and full experimental procedures. This material is available free of charge via the Internet at http://pubs.acs.org.

■ AUTHOR INFORMATION

Corresponding Author
emilio.perez@imdea.org; nazmar@quim.ucm.es

■ ACKNOWLEDGMENT

■ REFERENCES

(1) Kroto, H. W.; Heath, J. R.; O'Brien, S. C.; Curl, R. F.; Smalley, R. E. *Nature* **1985**, *318*, 162.

(2) (a) Effing, J.; Jonas, U.; Jullien, L.; Plesnivy, T.; Ringsdorf, H.; Diederich, F.; Thilgen, C.; Weinstein, D. *Angew. Chem., Int. Ed. Engl.* **1992**, *31*, 1599. (b) Andersson, T.; Nilsson, K.; Sundahl, M.; Westman, G.; Wennerström, O. *Chem. Commun.* **1992**, 604.

(3) For reviews, see: (a) Pérez, E. M.; Martín, N. *Pure Appl. Chem.* **2010**, *82*, 523–533. (b) Pérez, E. M.; Martín, N. *Chem. Soc. Rev.* **2008**, *37*, 1512–1519. (c) Tashiro, K.; Aida, T. *Chem. Soc. Rev.* **2007**, *36*, 189–197. (d) Kawase, T.; Oda, M. *Pure Appl. Chem.* **2006**, *78*, 831–839. (e) Boyd, P. D. W.; Reed, C. A. *Acc. Chem. Res.* **2005**, *38*, 235–242. For recent examples, see:(f) Franco, J. U.; Hammons, J. C.; Rios, D.; Olmstead, M. M. *Inorg. Chem.* **2010**, *49*, 5120–5125. (g) Shoji, Y.; Tashiro, K.; Aida, T. *J. Am. Chem. Soc.* **2010**, *132*, 5928–5929. (h) Huerta, E.; Isla, H.; Pérez, E. M.; Bo, C.; Martín, N.; de Mendoza, J. *J. Am. Chem. Soc.* **2010**, *132*, 5351–5353. (i) Balandier, J.-Y.; Chas, M.; Dron, P. I.; Goeb, S.; Canevet, D.; Belyasmine, A.; Allain, M.; Sallé, M. *J. Org. Chem.* **2010**, *75*, 1589–1599. (j) Zhang, E.-X.; Wang, D.-X.; Zheng, Q.-Y.; Wang, M.-X.

Org. Lett. **2008**, *10*, 2565–2568. (k) Xiao, W.; Passerone, D.; Ruffieux, P.; Aiet-Mansour, K.; Gröning, O.; Tosatti, E.; Siegel, J. S.; Fasel, R. *J. Am. Chem. Soc.* **2008**, *130*, 4767–4771. (l) Pérez, E. M.; Capodilupo, A. L.; Fernández, G.; Sánchez, L.; Viruela, P. M.; Viruela, R.; Ortí, E.; Bietti, M.; Martín, N. *Chem. Commun.* **2008**, 4567–4569. (m) Marois, J.-S.; Cantin, K.; Desmarais, A.; Morin, J.-F. *Org. Lett.* **2008**, *10*, 33–36. (n) Liu, S.-Q.; Wang, D.-X.; Zheng, Q.-Y.; Wang, M.-X. *Chem. Commun.* **2007**, 3856–3858. (o) Pérez, E. M.; Sierra, M.; Sánchez, L.; Torres, M. R.; Viruela, R.; Viruela, P. M.; Ortí, E.; Martín, N. *Angew. Chem., Int. Ed.* **2007**, *46*, 1847–1851. (p) Sygula, A.; Fronczek, F. R.; Sygula, R.; Rabideau, P. W.; Olmstead, M. M. *J. Am. Chem. Soc.* **2007**, *129*, 3842–3843. (q) Huerta, E.; Metselaar, G. A.; Fragoso, A.; Santos, E.; Bo, C.; de Mendoza, J. *Angew. Chem., Int. Ed.* **2007**, *46*, 202–205. (r) Huerta, E.; Cequier, E.; de Mendoza, J. *Chem. Commun.* **2007**, 5016–5018. (s) Yanagisawa, M.; Tashiro, K.; Yamasaki, M.; Aida, T. *J. Am. Chem. Soc.* **2007**, *129*, 11912–11913. (t) Pérez, E. M.; Sánchez, L.; Fernández, G.; Martín, N. *J. Am. Chem. Soc.* **2006**, *128*, 7172–7173. (u) Hosseini, A.; Taylor, S.; Accorsi, G.; Armaroli, N.; Reed, C. A.; Boyd, P. D. W. *J. Am. Chem. Soc.* **2006**, *128*, 15903–15913. (v) Shoji, Y.; Tashiro, K.; Aida, T. *J. Am. Chem. Soc.* **2006**, *128*, 10690–10691.

(4) For a review on fullerene materials constructed by self-assembly, see: (a) Nakanishi, T. *Chem. Commun.* **2010**, *46*, 3425–3436. For selected recent examples, see: (b) Xue, P.; Lu, R.; Zhao, L.; Xu, D.; Zhang, X.; Li, K.; Song, Z.; Yang, X.; Takafuji, M.; Ihara, H. *Langmuir* **2010**, *26*, 6669–6675. (c) Haino, T.; Hirai, E.; Fujiwara, Y.; Kashihara, K. *Angew. Chem., Int. Ed.* **2010**, *49*, 7899–7903. (d) Zhang, X.; Takeuchi, M. *Angew. Chem., Int. Ed.* **2009**, *48*, 9646–9651. (e) D'Souza, F.; Maligaspe, E.; Ohkubo, K.; Zandler, M. E.; Subbaiyan, N. K.; Fukuzumi, S. *J. Am. Chem. Soc.* **2009**, *131*, 8787–8797. (f) Wang, J.; Shen, Y.; Kessel, S.; Fernandes, P.; Yoshida, K.; Yagai, S.; Kurth, D. G.; Mohwald, H.; Nakanishi, T. *Angew. Chem., Int. Ed.* **2009**, *48*, 2166–2170. (g) Tsunashima, R.; Noro, S.-i.; Akutagawa, T.; Nakamura, T.; Kawakami, H.; Toma, K. *Chem.—Eur. J.* **2008**, *14*, 8169–8176. (h) Nakanishi, T.; Michinobu, T.; Yoshida, K.; Shirahata, N.; Ariga, K.; Mohwald, H.; Kurth, D. G. *Adv. Mater.* **2008**, *20*, 443–446. (i) Fernández, G.; Sánchez, L.; Pérez, E. M.; Martín, N. *J. Am. Chem. Soc.* **2008**, *130*, 10674–10683. (j) Fernández, G.; Pérez, E. M.; Sánchez, L.; Martín, N. *J. Am. Chem. Soc.* **2008**, *130*, 2410–2411. (k) Fernández, G.; Pérez, E. M.; Sánchez, L.; Martín, N. *Angew. Chem., Int. Ed.* **2008**, *47*, 1094–1097. (l) Araki, Y.; Chitta, R.; Sandanayaka, A. S. D.; Langenwalter, K.; Gadde, S.; Zandler, M. E.; Ito, O.; D'Souza, F. *J. Phys. Chem. C* **2008**, *112*, 2222–2229. (m) Barrau, S.; Heiser, T.; Richard, F.; Brochon, C.; Ngov, C.; van de Wetering, K.; Hadziioannou, G.; Anokhin, D. V.; Ivanov, D. A. *Macromolecules* **2008**, *41*, 2701–2710. (n) Schmittel, M.; He, B.; Mal, P. *Org. Lett.* **2008**, *10*, 2513–2516. (o) Yoshimoto, S.; Tsutsumi, E.; Narita, R.; Murata, Y.; Murata, M.; Fujiwara, K.; Komatsu, K.; Ito, O.; Itaya, K. *J. Am. Chem. Soc.* **2007**, *129*, 4366–4376. (p) Wessendorf, F.; Gnichwitz, J.-F.; Sarova, G. H.; Hager, K.; Hartnagel, U.; Guldi, D. M.; Hirsch, A. *J. Am. Chem. Soc.* **2007**, *129*, 16057–16071. (q) Zhong, Y.-W.; Matsuo, Y.; Nakamura, E. *J. Am. Chem. Soc.* **2007**, *129*, 3052–3053. (r) Hahn, U.; Gegout, A.; Duhayon, C.; Coppel, Y.; Saquet, A.; Nierengarten, J.-F. *Chem. Commun.* **2007**, 516–518. (s) Bonifazi, D.; Kiebele, A.; Stohr, M.; Cheng, F.; Jung, T.; Diederich, F.; Spillmann, H. *Adv. Funct. Mater.* **2007**, *17*, 1051–1062. (t) Pan, G.-B.; Cheng, X.-H.; Hoeger, S.; Freyland, W. *J. Am. Chem. Soc.* **2006**, *128*, 4218–4219.

(5) (a) Nielsen, K. A.; Sarova, G. H.; Martín-Gomis, L.; Fernández-Lazaro, F.; Stein, P. C.; Sanguinet, L.; Levillain, E.; Sessler, J. L.; Guldi, D. M.; Sastre-Santos, A.; Jeppesen, J. O. *J. Am. Chem. Soc.* **2008**, *130*, 460–462. (b) Haino, T.; Matsumoto, Y.; Fukazawa, Y. *J. Am. Chem. Soc.* **2005**, *127*, 8936–8937. (c) Haino, T.; Yanase, M.; Fukunaga, C.; Fukazawa, Y. *Tetrahedron* **2006**, *62*, 2025–2035. (d) Haino, T.; Fukunaga, C.; Fukazawa, Y. *Org. Lett.* **2006**, *8*, 3545–3548. (e) Haino, T.; Araki, H.; Fujiwara, Y.; Tanimoto, Y.; Fukazawa, Y. *Chem. Commun.* **2002**, 2148–2149. (f) Haino, T.; Yanase, M.; Fukazawa, Y. *Angew. Chem., Int. Ed.* **1998**, *37*, 997–998. (g) Haino, T.; Yanase, M.; Fukazawa, Y. *Angew. Chem., Int. Ed.* **1997**, *36*, 259–260. (h) Wu, J.-C.; Wang, D.-X.; Huang, Z.-T.; Wang, M.-X. *Tetrahedron Lett.* **2009**, *50*, 7209–7212. (i) Raston, C. L.; Atwood, J. L.; Nichols, P. J.; Sudria, I. B. N. *Chem.*

Commun. **1996**, 2615–2616. (j) Araki, K.; Akao, K.; Ikeda, A.; Suzuki, T.; Shinkai, S. *Tetrahedron Lett.* **1996**, *37*, 73–76.

(6) (a) Rio, Y.; Nierengarten, J.-F. *Tetrahedron Lett.* **2002**, *43*, 4321–4324. (b) Felder, D.; Heinrich, B.; Guillon, D.; Nicoud, J.-F.; Nierengarten, J.-F. *Chem.—Eur. J.* **2000**, *6*, 3501–3507. (c) Nierengarten, J.-F.; Oswald, L.; Eckert, J.-F.; Nicoud, J.-F.; Armaroli, N. *Tetrahedron Lett.* **1999**, *40*, 5681–5684. (d) Matsubara, H.; Shimura, T.; Hasegawa, A.; Semba, M.; Asano, K.; Yamamoto, K. *Chem. Lett.* **1998**, 1099–1100. (e) Atwood, J. L.; Barnes, M. J.; Gardiner, M. G.; Raston, C. L. *Chem. Commun.* **1996**, 1449–1450. (f) Steed, J. W.; Junk, P. C.; Atwood, J. L.; Barnes, M. J.; Raston, C. L.; Burkhalter, R. S. *J. Am. Chem. Soc.* **1994**, *116*, 10346–10347.

(7) (a) Mueck-Lichtenfeld, C.; Grimme, S.; Kobryn, L.; Sygula, A. *Phys. Chem. Chem. Phys.* **2010**, *12*, 7091–7097. (b) Georghiou, P. E.; Tran, A. H.; Mizyed, S.; Bancu, M.; Scott, L. T. *J. Org. Chem.* **2005**, *70*, 6158–6163. (c) Mizyed, S.; Georghiou, P.; Bancu, M.; Cuadra, B.; Rai, A. K.; Cheng, P.; Scott, L. T. *J. Am. Chem. Soc.* **2001**, *123*, 12770–12774.

(8) (a) Kawase, T.; Kurata, H. *Chem. Rev.* **2006**, *106*, 5250–5273. (b) Kawase, T.; Tanaka, K.; Shiono, N.; Seirai, Y.; Oda, M. *Angew. Chem., Int. Ed.* **2004**, *43*, 1722–1724. (c) Kawase, T.; Fujiwara, N.; Tsutumi, M.; Oda, M.; Maeda, Y.; Wakahara, T.; Akasaka, T. *Angew. Chem., Int. Ed.* **2004**, *43*, 5060–5062. (d) Kawase, T.; Tanaka, K.; Seirai, Y.; Shiono, N.; Oda, M. *Angew. Chem., Int. Ed.* **2003**, *42*, 5597–5600.

(9) (a) Sato, H.; Tashiro, K.; Shinmori, H.; Osuka, A.; Murata, Y.; Komatsu, K.; Aida, T. *J. Am. Chem. Soc.* **2005**, *127*, 13086–13087. (b) Shoji, Y.; Tashiro, K.; Aida, T. *J. Am. Chem. Soc.* **2004**, *126*, 6570–6571. (c) Ayabe, M.; Ikeda, A.; Kubo, Y.; Takeuchi, M.; Shinkai, S. *Angew. Chem., Int. Ed.* **2002**, *41*, 2790–2792. (d) Sun, D.; Tham, F. S.; Reed, C. A.; Chaker, L.; Boyd, P. D. W. *J. Am. Chem. Soc.* **2002**, *124*, 6604–6612. (e) Kubo, Y.; Sugasaki, A.; Ikeda, M.; Sugiyasu, K.; Sonoda, K.; Ikeda, A.; Takeuchi, M.; Shinkai, S. *Org. Lett.* **2002**, *4*, 925–928. (f) Zheng, J.-Y.; Tashiro, K.; Hirabayashi, Y.; Kinbara, K.; Saigo, K.; Aida, T.; Sakamoto, S.; Yamaguchi, K. *Angew. Chem., Int. Ed.* **2001**, *40*, 1857–1861.

(10) Gil-Ramírez, G.; Karlen, S. D.; Shundo, A.; Porfyrakis, K.; Ito, Y.; Briggs, G. A. D.; Morton, J. J. L.; Anderson, H. L. *Org. Lett.* **2010**, *12*, 3544–3547.

(11) Song, J.; Aratani, N.; Shinokubo, H.; Osuka, A. *J. Am. Chem. Soc.* **2010**, *132*, 16356–16357.

(12) Isla, H.; Gallego, M.; Pérez, E. M.; Viruela, R.; Ortí, E.; Martín, N. *J. Am. Chem. Soc.* **2010**, *132*, 1772–1773.

(13) Continous variation plots to confirm the stoichiometries of the associates were also carried out. For the sake of brevity, only those indicating 2:1 stoichiometry are shown. The Job's plot of *p*-**xylmac12** vs C_{60} can bee seen in ref 12.

(14) Minimizations were carried out utilizing the AMBER force field included in the HyperChem molecular modelling system. The AMBER force field was selected because it includes a term for van der Waals and electrostatic interactions. See: Cornell, W. D.; Cieplak, P.; Bayly, C. I.; Gould, I. R.; Merz, K. M., Jr.; Ferguson, D. M.; Spellmeyer, D. C.; Fox, T.; Caldwell, J. W.; Kollman, P. A. *J. Am. Chem. Soc.* **1995**, *117*, 5179. In the case of *p*-**xylmac12**, we have previously reported calculations at the DFT (BH&H/6-31G**) level (see ref 12). Because of the size of the collection of macrocycles, in this case we have resorted to less demanding molecular mechanics. The geometry optimization yields nearly identical results with both approaches. All optimizations were carried out with the *E* isomer of the corresponding macrocycle. We have previously shown that there is hardly any difference between the cavities of the *E* and *Z* macrocycles (see ref 12).

(15) Mizyed, S.; Georghiou, P. E.; Ashram, M. *J. Chem. Soc., Perkin Trans. 2* **2000**, 277–280.

(16) Semenov, K. N.; Charykov, N. A.; Keskinov, V. A.; Piartman, A. K.; Blokhin, A. A.; Kopyrin, A. A. *J. Chem. Eng. Data* **2010**, *55*, 13–36.

(17) Calix[4]pyrrole shows log K_a = 6.2 and 5.8 toward C_{70} in CHCl$_3$ and *o*-DCB, respectively: Pal, D.; Goswami, D.; Nayak, S. K.; Chattopadhyay, S.; Bhattacharya, S. *J. Phys. Chem. A* **2010**, *114*, 6776–6786.